The structure of a pentachromium(II) extended metal atom chain at 3 K: Cotton's conjecture proven / Cornia, Andrea; Nicolini, Alessio; Mcmonagle, Charles J.; Probert, Michael R.. - In: DALTON TRANSACTIONS. - ISSN 1477-9226. - 51:44(2022), pp. 16790-16794. [10.1039/D2DT03103E]

# The structure of a pentachromium(II) extended metal atom chain at 3 K: Cotton's conjecture proven

Andrea Cornia,*[a] Alessio Nicolini,[a] Charles J. McMonagle‡[b] and Michael R. Probert*[b]

[a]*Department of Chemical and Geological Sciences, University of Modena and Reggio Emilia & INSTM, I-41125 Modena, Italy.*
*E-mail: acornia@unimore.it*
[b]*Chemistry, School of Natural and Environmental Sciences, Newcastle University, Newcastle upon Tyne NE1 7RU, UK.*
*E-mail: Michael.Probert@newcastle.ac.uk*

**Abstract.** We provide definitive experimental proof that the archetypal string-like compound [$Cr_5(tpda)_4(NCS)_2$] has alternating long and short Cr-Cr separations in the solid state, as conjectured by F. A. Cotton, rather than essentially equally spaced Cr atoms, as initially claimed ($H_2$tpda = $N^2$,$N^6$-di(pyridin-2-yl)pyridine-2,6-diamine). Single-crystal X-ray data collected from 292 to 3 K revealed that the misinterpretation is caused by pseudo-merohedral twinning and that bond length alternation is enhanced at low temperature.

**Keywords**: chromium, cryo-crystallography, extended metal atom chains, twinning

†Electronic supplementary information (ESI) available: Synthetic and crystallographic details, additional plots of temperature-dependent structural parameters. CCDC 2208665-2208669 (**2**). For ESI and crystallographic data in CIF or other electronic format see DOI: https://doi.org/10.1039/XXX

‡Present address: Swiss-Norwegian Beam Lines (SNBL) at ESRF, 38043 Grenoble Cedex 9, France.

Arrays of closely spaced metal ions lined up into wire-like structures are known as extended metal atom chains (EMACs)[1] and have been the focus of intense investigation over the past two decades.[2–7] This linear topology is often assembled using specifically designed organic ligands, like fully deprotonated oligo-α-pyridylamines in the all-*syn* conformation, and may lead to the formation of metal-metal bonds.[8,9] The structural resemblance of EMACs to macroscopic wires and the possibility of a strong electronic communication among metal centers have suggested the possible use of these species as nanoscale wires in molecular electronics.[10–14] In this respect, chromium(II)-based EMACs are of special interest, since they display the highest molecular conductance among strings of the same nuclearity.[10,12] However, their geometrical and electronic features, and above all the actual extent of bond delocalization, have long been controversial.

A particularly lively debate arose around the X-ray structure of pentachromium(II) EMACs $[Cr_5(tpda)_4X_2]$, which contain four dianions of $N^2$,$N^6$-di(pyridin-2-yl)pyridine-2,6-diamine ($H_2$tpda) and X = $Cl^-$ (**1**) or $SCN^-$ (**2**) as capping ligands. The first compound of this family, **1**$\cdot CH_2Cl_2$, was reported by F. A. Cotton *et al.* in 1999.[15] Working on single-crystal X-ray data collected at 213 K, the authors noted that refinement of the five metal centers as full-occupancy scatterers afforded roughly equal Cr-Cr distances. However, the second and the fourth Cr atom had distinctly prolate displacement ellipsoids along the chain.[15] Such abnormal behaviour went unnoticed by S.-M. Peng's group, who shortly after claimed the occurrence of evenly spaced metals and delocalized metal-metal bonds in compounds **1**$\cdot 2Et_2O\cdot 4CHCl_3$ and isothiocyanate-capped **2**.[16] According to the interpretation proposed by Cotton's group, the elongated ellipsoids reflect unresolved disorder involving unsymmetrical chains with alternating short ($d_<$) and long ($d_>$) Cr-Cr separations.[15] Three additional sets of X-ray data collected on **1**$\cdot 2Et_2O\cdot 4CHCl_3$,[17] **1**$\cdot Et_2O$,[17] and **2**$\cdot 2.5CH_2Cl_2$[18] were later found consistent with the above model, showing that $d_<$ = 1.86-2.07 Å and $d_>$ = 2.50-2.66 Å in known solvatomorphs of **1** and **2** at 213 K. Based on Cotton's conjecture, then, these pentanuclear strings contain two pairs of quadruply bonded $Cr_2^{4+}$ units *plus* a virtually isolated $Cr^{2+}$ ion. The longer heptachromium(II) congener of **1**[19] as well as penta-,[20] hepta-,[21] and nonachromium[22] species with pyrazine-modulated ligands showed similar features.

This dual interpretation of X-ray data is presumably at the origin of the claimed existence of both symmetric *and* unsymmetric forms[12,23,24] to explain some electric and spectroscopic data. For instance, the bimodal single-molecule conductance of **2** measured in break-junction experiments[12] was attributed to coexisting symmetric and unsymmetric isomers. Similarly, from surface-enhanced Raman spectra it was inferred that **1** and **2** graft to metal nanoparticles in both symmetric and unsymmetric forms, with the former claimed as more stable.[23] While the existence of symmetric isomers in specific environments cannot be ruled out, density functional theory (DFT) calculations have provided an important hint in favour of Cotton's conjecture. Gas-phase studies indicate that the unsymmetric forms of **1** and **2** ($d_>$ = 2.55-2.61 Å, $d_<$ = 1.86-1.91 Å) are more stable than the symmetric structures by 2.9 and 1.7 kcal $mol^{-1}$, respectively, although with a shallow potential energy surface.[25,26] Inclusion of implicit solvent ($CH_2Cl_2$) effects renders the unsymmetric structure of **1** even slightly more favoured over the symmetric form.[25] In the case of trichromium(II) compound $[Cr_3(dpa)_4Cl_2]\cdot x Et_2O\cdot(1-x)CH_2Cl_2$ (**3**$\cdot x Et_2O\cdot(1-x)CH_2Cl_2$) a similar controversy was experimentally solved by following the structure down to 15 K (Hdpa = dipyridin-2-yl-amine). This showed that the central metal atom is not affected by static displacive disorder[27] but has large thermal vibrations.[28]

We herein provide direct validation of Cotton's conjecture for **2** by presenting its temperature-dependent solid-state structure down to 3 K. This specific compound (for synthetic details see ESI†) was chosen primarily as it contains no lattice solvent and is best suited for cryo-crystallography. Additionally, it is one of the earliest reported pentachromium(II) strings[16] and was not reinvestigated by Cotton's group. Its crystal structure was originally solved and refined in tetragonal space-group *I*4/*m*, with the central metal (Cr3) residing on a 4/*m* symmetry site.[16] The crystallographically imposed centrosymmetry then implied massive disorder effects between left- and right-handed helices. The final model presented in Fig. 2 of Ref.[16] is indeed flawed by large displacement parameters and severe distortion of the ligand's skeleton. Similar difficulties in structure refinement where encountered with the reportedly tetragonal diethylether solvate $\mathbf{1}\cdot Et_2O$.[17]

Five X-ray diffraction datasets were collected on a single crystal of **2** from 292 to 3 K, utilising the XIPHOS diffraction facility[29] and in the following order: 292 K (denoted as 292 K *before*), 3 K, 15 K, 100 K, and 292 K. The observed diffraction patterns could be explained by a *C*-centered monoclinic lattice with $a \approx c$, $\beta \approx 90°$, and two pseudo-merohedral twin domains similar in size and rotated by 90° along *y* unique axis, so as to yield apparent fourfold symmetry (for details see ESI†). The unit cell parameters so obtained are gathered in Table 1. At all temperatures, the values of *a* and *c* differ by less than 0.1 Å and $\beta$ departs by less than 0.03° from 90°. From 292 to 3 K the unit cell volume shrinks by ca. 3%, primarily due to a contraction of **a** and **c** axes by 1.2-1.5%.

Refinement was indeed highly successful in space group *C*2/*c* (Table S1†) and afforded completely ordered structures with twin fractions close to 0.5:0.5 (Table 1). The unit cell comprises four pentachromium(II) molecules ($Z = 4$). In each molecule, the four $tpda^{2-}$ ligands are helically wrapped around the five metal centers, with the isothiocyanato ligands axially bound to the two terminal Cr atoms (Cr1 and Cr5). All metal atoms and all atoms of isothiocyanato ligands lie on a twofold crystal axis parallel to *y*, resulting in a perfectly linear SCN–Cr–Cr–Cr–Cr–Cr–NCS moiety. This $C_2$ crystallographic symmetry is consistent with the EPR spectra of **2**,[26] which can only be accurately fitted by including a small rhombic anisotropy term that would be forbidden in a fourfold symmetric molecule.[16]

Most important, no disorder between left- and right-handed helices is detected and the arrangement of Cr centers along the chain is markedly unsymmetric even close to room temperature. These observations prove that the "averaged" structure with approximately evenly spaced metals reported by Peng's group[16] is a consequence of unaccounted for twinning rather than unresolved disorder effects.[30]

**Table 1** Unit cell parameters (Å, deg, Å$^3$) and twin fractions in **2** at different temperatures (K).

| $T$ | $a$ | $b$ | $c$ | $\alpha$ | $\beta$ | $\gamma$ | $V_c$ | Twin fractions |
|---|---|---|---|---|---|---|---|---|
| 292$^a$ | 15.2547(4) | 26.2195(8) | 15.2032(4) | 90 | 90.0121(16) | 90 | 6080.8(3) | 0.558(3):0.442(3) |
| 3 | 15.0605(4) | 26.1672(7) | 14.9728(4) | 90 | 90.023(2) | 90 | 5900.6(3) | 0.549(2):0.451(2) |
| 15 | 15.0601(4) | 26.1633(7) | 14.9768(4) | 90 | 90.0266(16) | 90 | 5901.2(3) | 0.542(2):0.458(2) |
| 100 | 15.1037(4) | 26.1632(8) | 15.0198(4) | 90 | 90.0189(16) | 90 | 5935.2(3) | 0.570(2):0.430(2) |
| 292$^b$ | 15.2426(3) | 26.2039(7) | 15.2056(3) | 90 | 90.0060(10) | 90 | 6073.4(2) | 0.575(3):0.425(3) |

$^a$Before cooling down. $^b$After cooling down.

The 292 K structure is depicted in Fig. 1a along with the adopted atom labelling scheme, which identifies Cr1 as the "isolated" metal center. At this temperature, $d_>$ and $d_<$ are in the range 2.40-2.42 Å and 2.09-2.15 Å, respectively, with Cr1-Cr2 slightly longer than Cr3-Cr4 by 0.02 Å and Cr4-Cr5 exceeding Cr2-Cr3 by 0.06 Å (Table 2). Upon cooling from 292 to 3 K, the **b** axis shortens by less than 0.2% (Table 1) whereas the Cr-Cr distances undergo significantly larger variations (Fig. 1b and Table 2). As graphically shown in Fig. 2, the $d_>$ values increase by ca. 0.09-0.11 Å and converge to 2.51 Å, while the $d_<$ values decrease in a virtually parallel fashion by 0.10-0.11 Å and still differ by 0.06 Å at 3 K. The bond alternation parameter $\Delta d = d_> - d_<$, evaluated from the average values of $d_>$ and $d_<$, increases from 0.29 Å at 292 K to 0.49 Å at 3 K, although it remains smaller than predicted by DFT calculations (Table 2).[26] Notice that these geometrical changes take place mostly between 292 and 100 K, while the Cr-Cr distances undergo only minor variations below 100 K (~0.01 Å).

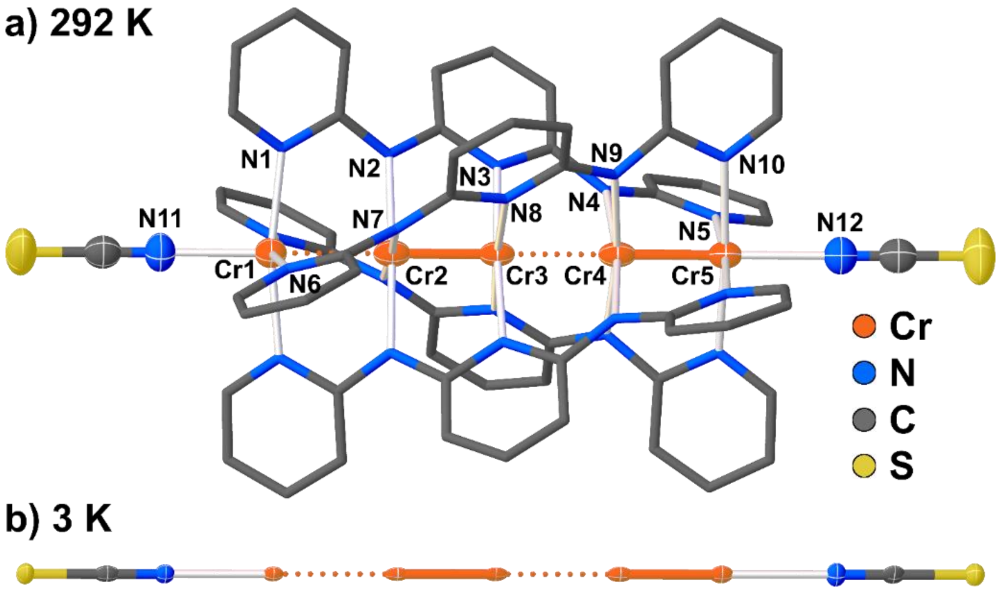

**Fig. 1** Molecular structure of **2** at 292 K (a) and 3 K (b). Displacement ellipsoids are set at 50% probability level. H atoms and (in the 3 K structure) tpda$^{2-}$ ligands are omitted.

As a result of molecular unsymmetry, Cr1-N11 and Cr5-N12 distances with isothiocyanato ligands also differ, the former being shorter by 0.09 Å at 292 K (Table 2). Upon cooling, the two bond lengths undergo small but significant changes in opposite directions, which cause the unsymmetry to reach 0.12 Å between 100 and 3 K. Such variations correlate with changes in the Cr-Cr distances: Cr1-N11 bond slightly shortens as Cr1-Cr2 interaction becomes concomitantly weaker, while Cr5-N12 distance increases slightly as Cr4-Cr5 interaction strengthens.

**Table 2** Selected interatomic distances and average Δ*d* values (Å) in **2** at different temperatures (K).

| *T* | Cr1-N11[a] | Cr1-Cr2 | Cr2-Cr3 | Cr3-Cr4 | Cr4-Cr5 | Cr5-N12[a] | Δ*d*[b] |
|---|---|---|---|---|---|---|---|
| 292[c] | 2.215(5) | 2.4198(12) | **2.0939(13)** | 2.4005(13) | **2.1541(12)** | 2.304(5) | 0.29 |
| 3 | 2.189(4) | 2.5061(10) | **1.9884(10)** | 2.5073(11) | **2.0500(10)** | 2.316(4) | 0.49 |
| 15 | 2.191(4) | 2.4969(10) | **1.9978(11)** | 2.4973(11) | **2.0589(10)** | 2.313(4) | 0.47 |
| 100 | 2.188(4) | 2.4954(10) | **1.9994(11)** | 2.4940(11) | **2.0609(10)** | 2.312(4) | 0.46 |
| 292[d] | 2.207(4) | 2.4167(10) | **2.0940(11)** | 2.3990(11) | **2.1517(10)** | 2.304(4) | 0.28 |
| DFT[e] | 2.053 | 2.547 | **1.865** | 2.604 | **1.908** | 2.156 | 0.69 |

[a] Nitrogen donor of isothiocyanato ligand. [b] Calculated as $\Delta d = d_> - d_<$ using average $d_>$ and $d_<$ values. [c] Before cooling down. [d] After cooling down. [e] From gas-phase DFT calculations in Ref. [26]

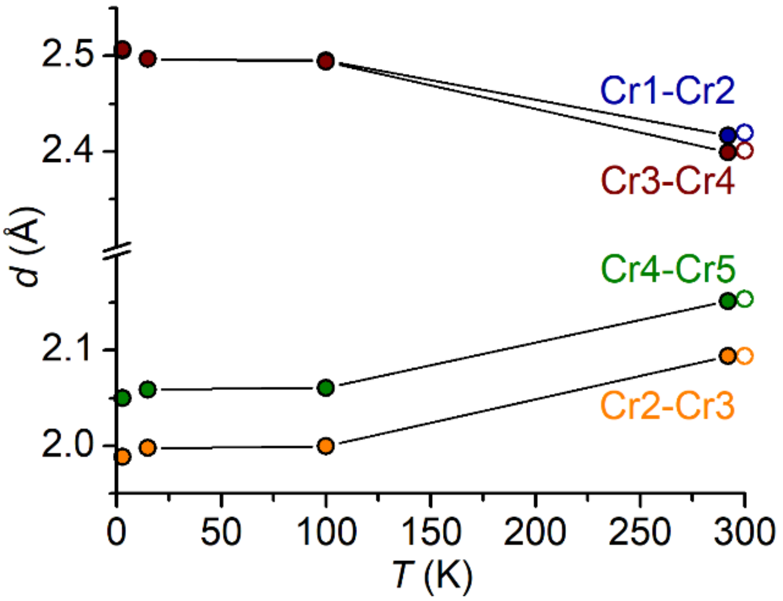

**Fig. 2** Temperature dependence of Cr-Cr distances in **2**. Empty circles are measurements at 292 K *before cooling down* (symbols have been moved slightly to the right for clarity). The error bars are within the size of the circles.

Turning to the metal coordination environments, the terminal metals Cr1 and Cr5 have idealized square pyramidal CrN$_5$ geometry, whereas the inner metals Cr2, Cr3, and Cr4 are in idealized CrN$_4$ square planar coordination. Cr-N distances and N-Cr-N angles not involving the terminal isothiocyanato ligands undergo only marginal variations from 292 to 3 K (Fig. S1† and Table S2†). At 292 K, the “isolated” metal Cr1 is located ca. 0.21 Å off its basal plane defined by the four N donors of tpda$^{2-}$ ligands, towards the apical SCN$^{-}$ ligand (Table S3†). Deviations of Cr2 and Cr3 from their coordination planes are small (0.04-0.06 Å) and in opposite directions, as a consequence of Cr2-Cr3 bonding. Cr4 is also off plane by 0.14 Å towards the neighbouring terminal metal Cr5. The latter lies much closer (0.07 Å) to its basal plane than Cr1 does, presumably because of the compensating Cr-Cr and Cr-NCS axial interactions. As temperature is lowered, the enhanced bond length alternation causes these deviations to increase for all ions except Cr5, which is pulled towards Cr4 and approaches its basal coordination plane even further (0.03 Å deviation at 3 K). The opposite temperature dependence of Cr1 and Cr5 coordination geometries is also evident by inspecting N-Cr1-N11 and N-Cr5-N12 angles (Fig. S1b†).

We now analyse the mean-square atomic displacements $U_{ij}$ for the five metals and for the isothiocyanato donor atoms N11 and N12 in **2** (Table S4† and Fig. S2a-c†). It is first worth noting that all metals in **2** have the *largest* mean-square displacement amplitude along the chain axis ($y$). For this reason, we herein focus on $U_{22}$ and on the average $U$-component transverse to $y$ ($U_t$). Fig. 3 shows that the mean-square displacement amplitudes $U_{22}$ vary significantly along the chain and that the following ordering holds at all temperatures: $U_{22}$(Cr1) < $U_{22}$(Cr5) < $U_{22}$(Cr3) < $U_{22}$(Cr2) $\lesssim$ $U_{22}$(Cr4). Thus, the two terminal metals (Cr1 and Cr5) and the inner metals Cr2 and Cr4 have the smallest and the largest $U_{22}$ values, respectively, among metal atoms. By contrast, $U_t$ increases smoothly when moving from the centre to the extremes of the molecule (Fig. S2d†). With decreasing temperature, both $U_{22}$ and $U_t$ drop considerably while the prolateness of all Cr displacement ellipsoids ($U_{22}/U_t$) is enhanced (Fig. S3a†). The reason is that $U_{22}$ parameters remain significant at 3 K (180-290·10$^{-4}$ Å$^2$) and much larger than found in **3** (<100·10$^{-4}$ Å$^2$ at 15 K).[28] The low-temperature differences $|\Delta U_{22}|$ between neighbouring metals also vary over a considerably larger interval than in **3** (20-100·10$^{-4}$ Å$^2$ vs. <30·10$^{-4}$ Å$^2$ at 15 K),[28] with the Cr1-Cr2 and Cr4-Cr5 pairs exhibiting the most negative and most positive $\Delta U_{22}$ values, respectively (Fig. S3b†).

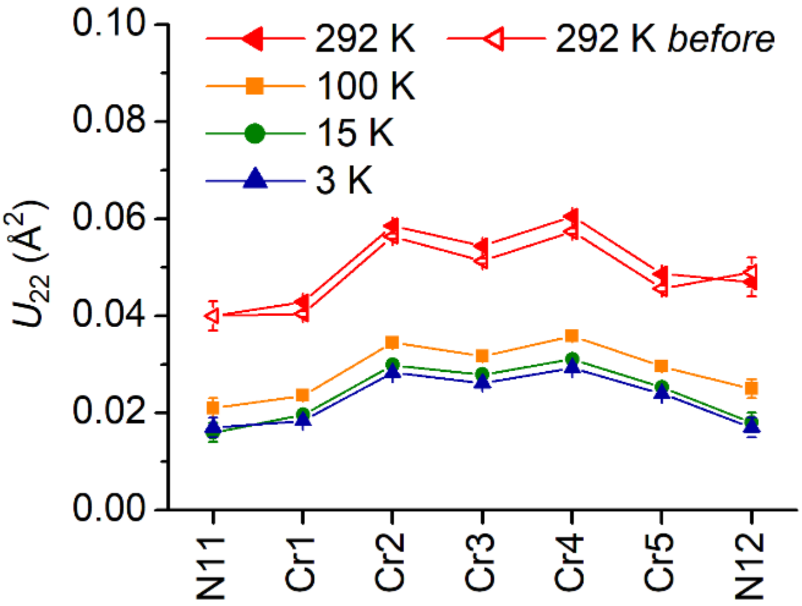

**Fig. 3** *U*-component along the chain axis for metal atoms, N11, and N12 in **2** at different temperatures.

These combined observations suggest that, in spite of the clear bond alternation, the metal atoms are affected by residual static displacive disorder,[27] which is more pronounced for the inner metals Cr2, Cr3, and Cr4. Such residual static distribution of metal positions is consistent with the very shallow potential energy surface evidenced by theoretical studies.[25,26]

As a final remark, we notice that N11 and Cr1 have virtually the same $U_{22}$ at all temperatures, suggesting that these two atoms undergo rigid-body displacements along the chain axis (Fig. 3). By contrast, $U_{22}$(N12) is within experimental error from $U_{22}$(Cr5) at 292 K, but slightly smaller at lower temperatures.

In summary, we have demonstrated that the pseudo-tetragonal diffraction symmetry of **2**, which led to structure analysis in space group *I*4/*m*,[16] is due to pseudo-merohedral twinning of *C*2/*c* domains. When twinning is properly considered, molecules of **2** are found unsymmetric in the solid state, with a clear alternation of long and short Cr-Cr separations. The observed unsymmetry matches the outcome of published DFT studies[25,26] and is enhanced at low temperature (3 K).

Crystal twinning occurs for precise structural reasons;[31] furthermore, the distinction between twinning and true disorder is determined by twin domain size vs. X-ray coherence length.[30] It is thus well possible that crystals of different pentachromium(II) compounds, like **2**·$2.5CH_2Cl_2$[18] or the three known solvates of chloride-capped **1**,[15,17] are best described as disordered assemblies of unsymmetric chains, as proposed by F. A. Cotton.

## Conflicts of interest

The authors declare no conflict of interest.

## Acknowledgements

This work was financially supported by Newcastle University and the EPSRC (grant EP/N01331X/1), and by the University of Modena and Reggio Emilia through a FAR2014 project. A.C. is grateful to S. Boccedi and R. Galavotti for their contributions to the synthesis of the compound.

## References

1 J. F. Berry, F. A. Cotton, L. M. Daniels, C. A. Murillo and X. Wang, *Inorg. Chem.*, 2003, **42**, 2418–2427.

2 G. Aromí, *Comments Inorg. Chem.*, 2011, **32**, 163–194.

3 S.-A. Hua, M.-C. Cheng, C. Chen and S.-M. Peng, *Eur. J. Inorg. Chem.*, 2015, **2015**, 2510–2523.

4 M.-C. Cheng, R.-X. Huang, Y.-C. Liu, M.-H. Chiang, G.-H. Lee, Y. Song, T.-S. Lin and S.-M. Peng, *Dalton Trans.*, 2020, **49**, 7299–7303.

5 K. Aoki, K. Otsubo, Y. Yoshida, Y. Kimura, K. Sugimoto and H. Kitagawa, *Inorg. Chem.*, 2021, **60**, 16029–16034.

6 A. Srinivasan, R. A. Musgrave, M. Rouzières, R. Clérac, J. E. McGrady and E. A. Hillard, *Chem. Commun.*, 2021, **57**, 13357–13360.

7 G. L. Guillet, K. Y. Arpin, A. M. Boltin, J. B. Gordon, J. A. Rave and P. C. Hillesheim, *Inorg. Chem.*, 2020, **59**, 11238–11243.

8 J. F. Berry, *Struct. Bond.*, 2010, **136**, 1–28.

9 S. Hua, Y. Tsai and S. Peng, *J. Chin. Chem. Soc.*, 2014, **61**, 9–26.

10 I.-W. P. Chen, M.-D. Fu, W.-H. Tseng, J.-Y. Yu, S.-H. Wu, C.-J. Ku, C. Chen and S.-M. Peng, *Angew. Chem. Int. Ed.*, 2006, **45**, 5814–5818.

11 P.-J. Chen, M. Sigrist, E.-C. Horng, G.-M. Lin, G.-H. Lee, C. Chen and S.-M. Peng, *Chem. Commun.*, 2017, **53**, 4673–4676.

12 T.-C. Ting, L.-Y. Hsu, M.-J. Huang, E.-C. Horng, H.-C. Lu, C.-H. Hsu, C.-H. Jiang, B.-Y. Jin, S.-M. Peng and C. Chen, *Angew. Chem. Int. Ed.*, 2015, **54**, 15734–15738.

13 V. P. Georgiev and J. E. McGrady, *J. Am. Chem. Soc.*, 2011, **133**, 12590–12599.

14 V. P. Georgiev, P. J. Mohan, D. DeBrincat and J. E. McGrady, *Coord. Chem. Rev.*, 2013, **257**, 290–298.

15 F. A. Cotton, L. M. Daniels, T. Lu, A. Murillo and X. Wang, *J. Chem. Soc., Dalton Trans.*, 1999, **5**, 517–518.

16 H. Chang, J. Li, C. Wang, T. Lin, H.-C. Lee, G. Lee and S. Peng, *Eur. J. Inorg. Chem.*, 1999, **1999**,

1243–1251.

17 F. A. Cotton, L. M. Daniels, C. A. Murillo and X. Wang, *Chem. Commun.*, 1999, **5**, 2461–2462.

18 J. F. Berry, F. A. Cotton, C. S. Fewox, T. Lu, C. a Murillo and X. Wang, *Dalton Trans.*, 2004, 2297–2302.

19 Y.-H. Chen, C.-C. Lee, C.-C. Wang, G.-H. Lee, S.-Y. Lai, F.-Y. Li, C.-Y. Mou and S.-M. Peng, *Chem. Commun.*, 1999, 1667–1668.

20 W.-Z. Wang, R. H. Ismayilov, G.-H. Lee, Y.-L. Huang, C.-Y. Yeh, M.-D. Fu, C. Chen and S.-M. Peng, *New J. Chem.*, 2012, **36**, 632–637.

21 R. H. Ismayilov, W.-Z. Wang, G.-H. Lee, C.-H. Chien, C.-H. Jiang, C.-L. Chiu, C.-Y. Yeh and S.-M. Peng, *Eur. J. Inorg. Chem.*, 2009, **2009**, 2110–2120.

22 R. H. Ismayilov, W.-Z. Wang, R.-R. Wang, C.-Y. Yeh, G.-H. Lee and S.-M. Peng, *Chem. Commun.*, 2007, 1121–1123.

23 Y.-M. Huang, H.-R. Tsai, S.-H. Lai, S. J. Lee, I.-C. Chen, C. L. Huang, S.-M. Peng and W.-Z. Wang, *J. Phys. Chem. C*, 2011, **115**, 13919–13926.

24 P. Gao, X.-P. Cai, Q. Xie, Q. Yang, H. Ou, W.-Q. Wu, X. Xu, Z. Xu and X. Lin, *Inorg. Chem.*, 2021, **60**, 9378–9386.

25 A. Dirvanauskas, R. Galavotti, A. Lunghi, A. Nicolini, F. Roncaglia, F. Totti and A. Cornia, *Dalton Trans.*, 2018, **47**, 585–595.

26 A. Cornia, A.-L. Barra, V. Bulicanu, R. Clérac, M. Cortijo, E. A. Hillard, R. Galavotti, A. Lunghi, A. Nicolini, M. Rouzières, L. Sorace and F. Totti, *Inorg. Chem.*, 2020, **59**, 1763–1777.

27 R. D. Poulsen, J. Overgaard, A. Schulman, C. Østergaard, C. A. Murillo, M. A. Spackman and B. B. Iversen, *J. Am. Chem. Soc.*, 2009, **131**, 7580–7591.

28 L.-C. Wu, M. K. Thomsen, S. R. Madsen, M. Schmoekel, M. R. V. Jørgensen, M.-C. Cheng, S.-M. Peng, Y.-S. Chen, J. Overgaard and B. B. Iversen, *Inorg. Chem.*, 2014, **53**, 12489–12498.

29 M. R. Probert, C. M. Robertson, J. A. Coome, J. A. K. Howard, B. C. Michell and A. E. Goeta, *J. Appl. Crystallogr.*, 2010, **43**, 1415–1418.

30 W. Massa, *Crystal Structure Determination*, Springer-Verlag, Berlin Heidelberg, 2nd edn., 2004.

31 R. Herbst-Irmer and G. M. Sheldrick, *Acta Crystallogr. Sect. B Struct. Sci.*, 1998, **54**, 443–449.